INSTITUTE OF PHYSICS PUBLISHING JOURNAL OF PHYSICS B: ATOMIC, MOLECULAR AND OPTICAL PHYSICS

J. Phys. B: At. Mol. Opt. Phys. **37** (2004) 3571–3581 PII: S0953-4075(04)80840-X

Differential and integrated cross sections for the electron excitation of the 4 ^{1}P^o state of calcium atom

S Milisavljević[1], D Šević[1], V Pejčev[1,2], D M Filipović[1,3] and B P Marinković[1]

[1] Institute of Physics, Belgrade, PO Box 68, 11080 Belgrade, Serbia and Montenegro
[2] Faculty of Natural Sciences, University of Kragujevac, Serbia and Montenegro
[3] Faculty of Physics, University of Belgrade, PO Box 368, 11001 Belgrade, Serbia and Montenegro

E-mail: bratislav.marinkovic@phy.bg.ac.yu

Received 13 May 2004
Published 6 September 2004
Online at stacks.iop.org/JPhysB/37/3571
doi:10.1088/0953-4075/37/18/002

Abstract

Differential cross section (DCS) data for excitation of the 4 ^{1}P^o state (2.93 eV) of Ca atoms by electrons have been obtained using a crossed electron–atom beam technique. The measurements were divided into two groups. The first one consists of measurements at 10, 20, 40, 60 and 100 eV impact electron energies from 1° to 10° scattering angle interval. The second group of measurements are those at larger scattering angles (10°–150°) at the same energies except 100 eV. Absolute values have been obtained by normalizing generalized oscillator strengths (GOS) to optical oscillator strength (OOS) in the minimum momentum transfer squared (K^2) limit. Integral, momentum transfer and viscosity cross sections have been determined from DCSs. A comparison is made with existing relativistic distorted wave calculation.

M This article features online multimedia enhancements

(Some figures in this article are in colour only in the electronic version)

1. Introduction

Electron-impact excitation cross sections for metal atoms are of great interest for many astrophysical and plasma problems such as observation, investigation, analysis and diagnostics of stellar spectra and laboratory plasma research and modelling [1–3]. Calcium is an alkaline earth atom with two 4s valence electrons outside an inert electron core. Calcium lines are prominent in solar and stellar spectra and cover a wide variety of line strengths and excitation conditions.

The first detailed study of calcium lines in the solar spectra was published by Holweger [4]. Many papers have been published in which the presence of Ca lines in solar and stellar spectra was confirmed. Calcium lines are very important for diagnostic purposes, especially for determinations of cool stellar atmospheric properties and for the study of chromospheric activity of late type stars [5, 6].

As is known, ultracold atoms could be important for many precision measurements. Due to applications in fields such as metrology, quantum optics, etc there are a lot of investigations whose main goal is development of new methods for the preparation of cold atoms. Calcium is of special interest for these purposes because of its strong resonance $^1S_0$–$^1P_1$ line, suitable for laser cooling. The spin forbidden $^1S_0$–$^3P_1$ narrow line (natural linewidth smaller than 400 Hz) is also interesting for many potential applications. Development of new generations of atomic frequency standards, i.e., clocks based on narrow optical lines of laser cooled neutral atoms, has been a field of extensive research in recent years. The aim is to reduce frequency noise level and amplitude, Doppler and Stark shifts etc using optical transitions instead of those in the radio frequency domain as in conventional atomic clocks. Work was focused on the intercombination $^1S_0$–$^3P_1$ calcium line at 657 nm which is extremely insensitive to different perturbations such as external fields, etc. Udem *et al* [7] presented results of absolute frequency measurements of both the H_g^+ and calcium optical standards. Oates *et al* [8, 9] reported an optical frequency standard based on this specific line of calcium. The group at PTB/Braunschweig performed high resolution spectroscopy measurements on laser cooled calcium [10–12], yielding data that could be used to obtain better accuracy in this direction. A review of investigations on frequency standards by Bauch and Telle [13] contains many data of interest for our investigation of calcium.

The calcium atom plays an important role in both experimental and theoretical studies of excitation and electron scattering by metal atoms with two valence electrons. Interest in these investigations has been growing in recent years. A few experimental studies are related to the $4\,^1P$ state of calcium. Work by Ehlers and Gallagher [14] made a major contribution to the investigation of the electron excitation process in calcium. They measured the excitation function and polarization of the $4\,^1P$ state for electron-impact energies from threshold to 1400 eV and also reported results for total electron excitation cross sections for this state. The first experimental coincidence study on the electron-impact excitation of the calcium atom was reported by Zohny *et al* [15]. Their results include the Stokes parameters and total polarization at an electron energy of 40 eV. Chwirot *et al* [16] presented the measured excitation parameters at an electron energy of 100 eV for six scattering angles between 10° and 45°. Dyl *et al* [17] also used an electron–photon coincidence technique but to obtain coherence parameters for electron impact excitation of the $4\,^1P_1$ state at 45 eV and 60 eV electron-impact energies and scattering angles between 15° and 40°. Law and Teubner [18] undertook a detailed investigation of the orientation of the $4\,^1P$ state in calcium using combined electron-impact and laser excitation in a superelastic electron scattering experiment. Orientation parameters were obtained for two energies (25.7 eV and 45 eV) and scattering angles from 3° to 100°. Recently, Murray and Cvejanović [19] obtained new superelastic scattering data for the same state in calcium. The radiation source used in this experiment was a high power CW:Ti: sapphire laser so it was possible to obtain results at energies ranging from 20 to 35 eV. Studies on calcium atoms include electron-impact ionization but there are only a few experimental works in this field. Cvejanović and Murray [20] measured relative cross sections for the single ionization of calcium in the energy range from threshold to 100.7 eV and the ion yield as a function of impact energy by using a time-of-flight method. The same group reported the first coplanar symmetric low-energy (e, 2e) measurements for calcium in which the electron-impact energy was changed from 10.1 to 64.6 eV [21]. Autoionization experiments on calcium were

conducted in the 3p autoionization region. In the electron-impact autoionization experiment by Pejčev *et al* [22] ejected-electron spectra (165 lines in the energy range 12.8 to 28.1 eV) of calcium for incident electron energies from 30 to 500 eV were reported. Feuerstein *et al* [23] measured the 3p ionization cross section of the diagram Auger states $3p^5 4s^2\, ^2P_{3/2}$ and $^2P_{1/2}$ and of specific satellite Auger states in the electron-impact energy range from threshold to 1.5 keV. There were also a few results obtained from photoionization experiments [24–26] using synchrotron radiation sources. The simultaneous ionization and excitation process was experimentally investigated by Hamdy *et al* [27] and recently by Stevenson and Crowe [28]. They presented results for emission cross sections and polarization for $4\,^2P_{3/2}$–$4\,^2S_{1/2}$ transition.

Srivastava *et al* [29] reported a calculation for the excitation of the $4\,^{1,3}P_1$ states of calcium based on the relativistic distorted-wave approximation, introduced by Zuo *et al* [30], for incident electron energies in the range from 20 to 100 eV. Results are presented for differential cross sections, generalized spin-polarization and electron–photon coherence parameters. Relativistic effects such as spin–orbit coupling of the excited atomic states are included, and distorted waves describing the scattered electron were calculated from the corresponding Dirac equation. Recently, Muktavat *et al* [31] extended these calculations to electron excitation of the ^{1,3}D states of calcium.

In this paper we present results of measurements of differential cross sections (DCS) for inelastic electron scattering by the Ca atom as well as integral (Q_I), momentum transfer (Q_M) and viscosity (Q_V) cross sections. We performed two series of measurements, one for electron-impact energies of 10, 20, 40, 60 and 100 eV at small scattering angles (1°–10°) and the other within a scattering angle interval from 10° to 150° at the same energies except 100 eV. Our results are presented on an absolute scale and compared with available theoretical data by Srivastava *et al* [29]. Integral cross sections are compared with results by Ehlers and Gallagher [14].

2. Experimental technique and procedure

The electron spectrometer for electron–metal-atom scattering used in this experiment has been described in detail by Predojević *et al* [32] and the experimental set-up is shown schematically in figure 1. In brief, the experiment was carried out by utilizing a crossed electron–atom beam technique. An energy selected electron beam (full width at half maximum (FWHM) around 100 meV) was perpendicularly crossed by an atomic beam and the angular distributions for the inelastically scattered electrons were measured at fixed impact energy E_0.

A hairpin thermoelectron source was used and an electron beam was formed by the electron monochromator which consists of systems of cylindrical electrostatic lenses and an hemispherical electrostatic energy selector. Electrons emitted from a hairpin cathode were extracted by a Pierce-type electrode (Pierce electrode in figure 1) and then electrons were collimated and decelerated (C_1, C_2 and D_{acc}). A Herzog electrode (H_1) was used to collimate electrons in the hemispherical energy selector. After that, electrons were passed through a second Herzog electrode (H_2) and then they were accelerated (A_{cc}) and focused (F_1) by a zoom lens to the interaction centre. The primary electron current was of the order of 10–50 nA, depending on the impact energy. Focusing properties and beam divergence enable high resolution measurements in the intermediate energy range. Transmission of the electron optics permits reliable results for electron-impact energies from 10 to 100 eV and residual electron energy above approximately 1 eV.

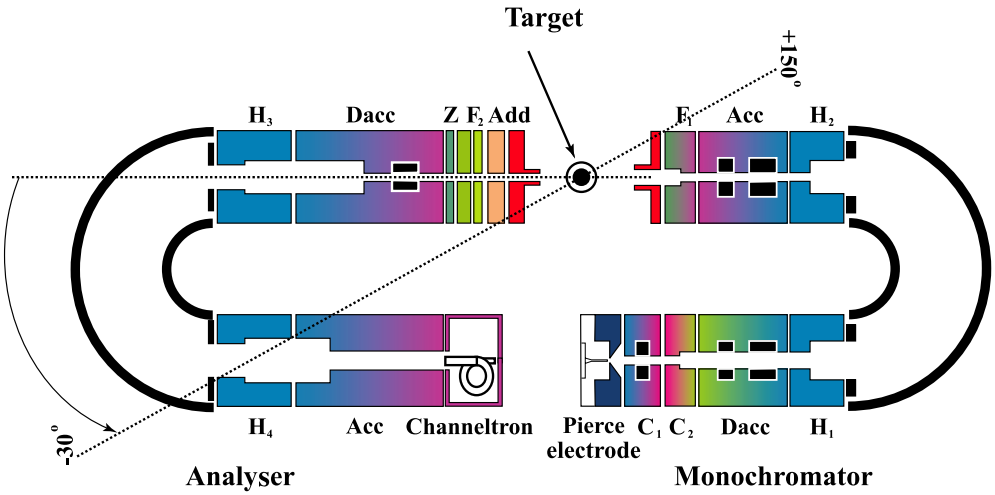

Figure 1. Schematic overview of hemispherical electron spectrometer: C, extracting electrode; D_{acc}, decelerating electrode; H, Herzog electrode; A_{cc}, accelerating electrode; F, focusing electrode.

Inelastically scattered electrons (electrons which had excited $4\,^1P^o$ state of calcium and therefore lost 2.93 eV of their energy) were detected by the hemispherical electron energy analyser with a channel electron multiplier (Channeltron) as a single-electron detector at the end. The analyser is of the same type as the monochromator and it can rotate around the atomic beam axis from –30° to 150° with respect to the incoming electron beam. At the analyser entrance, there is an 'energy add' lens (A_{dd}), which adds back to electrons the energy lost in the collision, and combined with the next zoom lens ensures that scattered electrons pass through the analyser like elastically scattered, i.e., ensures approximately constant electron transmission. At the end, electrons were focused onto the single-electron multiplier. All cylindrical lenses in the monochromator and analyser are made of gold-plated oxygen-free high conductivity copper while the hemispherical electrostatic energy selectors are made of molybdenum.

An atomic beam was produced by heating calcium (99.5% purity) in a wire-heating oven and was effused through a 20 mm long channel in the cap of the oven crucible which has an inner diameter of 1.5 mm. A diagram of the oven and exit aperture is shown in figure 2. The main modification to the usual setup is that the thicknesses of the oven walls were reduced and additional shielding was performed. This design permits higher temperatures to be achieved which provide vaporization of the calcium sample and ensure reliable work for extended periods of time. The oven was heated to about 700–720 °C by two separate heaters, one for the top of the stainless steel crucible and nozzle, and the other for the body of the crucible. They provided a variable temperature difference between the top and the bottom—the nozzle was maintained at approximately 100 °C higher temperature in order to prevent clogging. The heaters are wound in helical grooves on stainless steel heater bearings. The temperature of oven was controlled by two thermocouples, one installed at the top of the crucible and the other at the bottom. Contamination of the chamber was prevented with a liquid-nitrogen cold trap placed above the oven and interaction region. Transfer of heat and radiation losses from the oven are minimized and reduced by two (inner/outer) stainless steel shields located near the crucible and insulated by ceramics and a copper shield around the oven. Stainless steel screws adjusted the position of the oven. Overheating of the surrounding components was avoided by additional water-cooling.

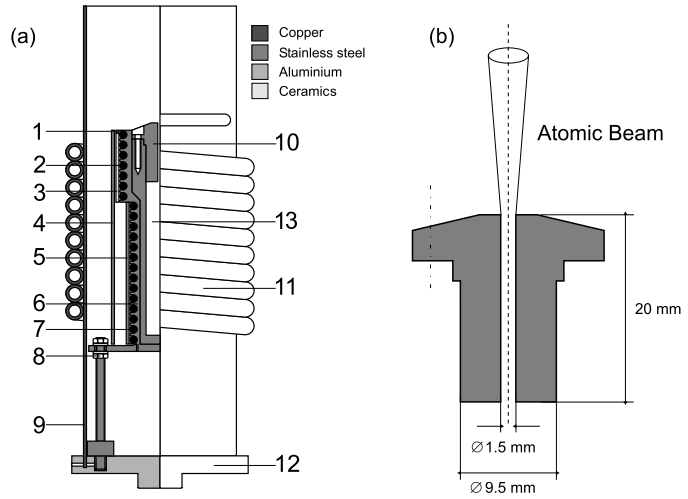

Figure 2. (a) Scaled diagram of the oven: (1) cover for ceramic shield; (2) heater; (3) ceramic shield; (4) stainless steel outer shield; (5) stainless steel inner shield; (6) stainless steel heater bearing; (7) heater; (8) stainless steel screws for height adjustment; (9) copper shield; (10) cap of the crucible; (11) water cooling; (12) oven holding plate; (13) crucible. (b) Cap of the crucible—exit aperture.

The energy scale was calibrated by measuring the position of the feature in the elastic scattering attributed to the threshold energy of the 4 ^{1}P^o excitation of calcium at 2.93 eV. An overall energy resolution of $\sim$160 meV was sufficient to resolve the resonant state and to ensure good working conditions. The angular resolution in the present experiment is checked and estimated to be 1.5° as it was in our previous experiment [32].

The experiment was conducted in a vacuum chamber, which was shielded by a double μ-metal shield so the magnetic field was below 2×10^{-7} T. Two oil diffusion pumps with liquid nitrogen traps provided differential pumping of the vacuum chamber and electron optics system. The background pressure was of the order of 10^{-5} Pa.

Before each measurement an energy loss spectrum was obtained to verify the absence of double scattering. This was achieved by searching for a peak at double resonant energy loss of 2×2.93 eV. Double scattering features were not observed at our working temperatures and therefore their effects and contribution to measured scattered electron intensities can be neglected. A typical energy loss spectrum is shown in figure 3. We performed decomposition of the feature at 2.93 eV whose profile is not symmetric. The 3 ^{1}D$_2$ and 3 ^{3}D$_{1,2,3}$ states are not completely resolved, but an energy resolution of 160 meV was sufficient to avoid their influence on measurements of the 4 ^{1}P^o state.

The position of true zero scattering angle was determined from the symmetry of the angular distribution of scattered electrons at negative and positive scattering angles. These measurements were carried out for scattered electrons in the range from –10° to +10° for each impact energy, and the angular scale was corrected. The associated error in angular scale determination was $\pm 0.2^\circ$. The scattered electron intensity was measured as a function of scattering angle. The analyser was adjusted to record only electrons that had lost 2.93 eV. These measurements were carried out in the full angle interval and then the detector was returned to a reference angle. In this way it was checked that the measurements were made under unchanged conditions.

The measured angular distributions were converted into relative DCSs by using the appropriate effective length correction factors. We have applied the correction factors of Brinkman and Trajmar [33], modified for our experimental conditions.

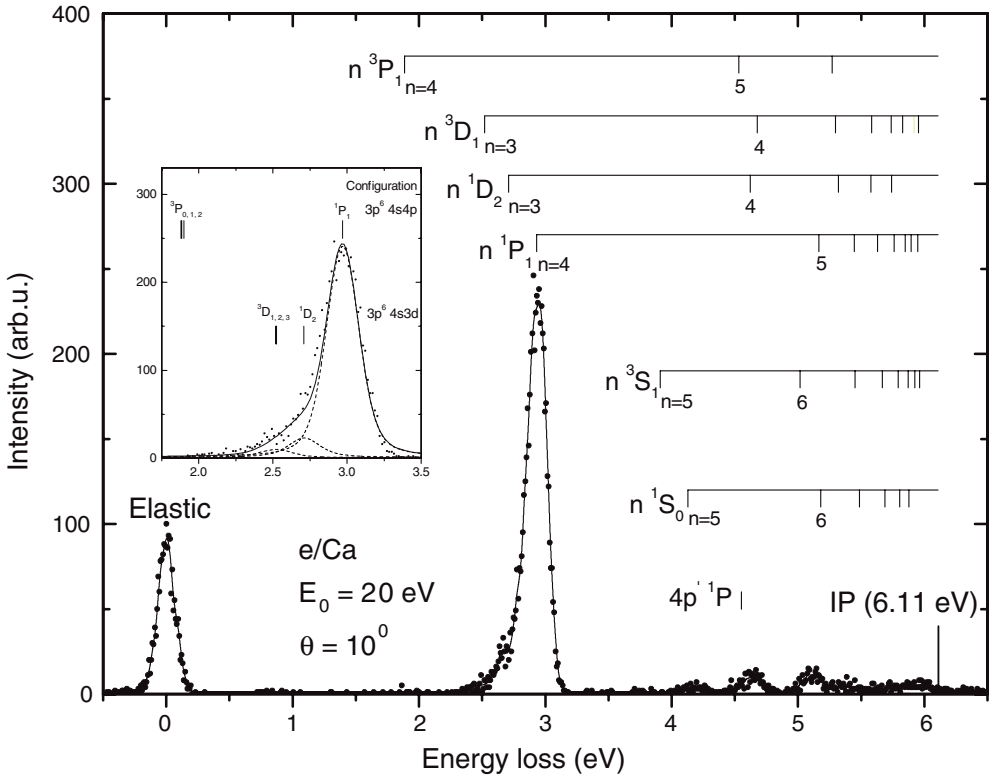

Figure 3. Energy loss spectrum of calcium at 20 eV electron-impact energy and 10° scattering angle. Decomposed energy loss spectrum near 2.93 eV is shown in inset: ●, measured intensity; ——, best fit; - - - -, decomposed states.

We normalized the relative DCSs as described by Felfli and Msezane [34]. Our preliminary results were presented earlier [35]. In order to put results on an absolute scale, relative DCSs were normalized through known values of the optical oscillator strength (OOS) by utilizing the forward scattering function (FSF) method [36] for generalized oscillator strengths (GOSs) of the 4 ^{1}P resonant state of calcium. This technique is based on the fact that GOS tends to OOS as momentum transfer squared (K^2) tends to zero. At each impact energy, the smallest value of K^2 was obtained for scattering angle $\theta = 0^\circ$. Fitted results were extrapolated to 0° scattering angle and the corresponding GOS was normalized to the forward scattering function. Normalization factors obtained in this way were used to put cross sections on an absolute scale. Absolute DCSs were extrapolated to 0° and 180° and then integrated to obtain integral, momentum transfer and viscosity cross sections.

3. Results and discussion

We have measured the angular distribution of electrons inelastically scattered by calcium atoms for the 4 ^{1}P^o state at 10, 20, 40, 60 eV and 100 eV electron impact energies. The scattering intensities were recorded from 10° to 150° in 10° increments and from 1° to 10° at each 1°. Small scattering angles are relevant for the normalization procedure. The measurements at 100 eV impact energy were done only at small scattering angles. GOS values for the 4 ^{1}P^o

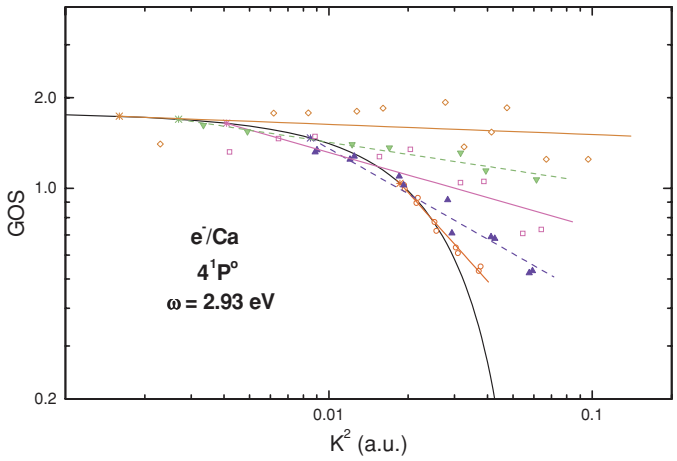

Figure 4. Generalized oscillator strengths (GOS) for the 4 ^{1}P^o state of the calcium atom versus momentum transfer squared (K^2): ○, 10 eV; ▲, 20 eV; □, 40 eV; ▼, 60 eV; ◇, 100 eV electron-impact energies with corresponding fitting curves; ∗, the appropriate minimal values of K^2; ——, forward scattering function (FSF) generated using the experimental optical oscillator strength (OOS) value of 1.79 ± 0.03 obtained by Kelly and Mathur [37].

M A supplementary data table is available online at stacks.iop.org/JPhysB/37/3571

state of the calcium atom are shown in figure 4 as a function of K^2 together with FSF which is obtained according to the experimental OOS of 1.79 ± 0.03 by Kelly and Mathur [37].

The position of the squared momentum transfer minimum moves to a smaller value if the electron energy increases, from 0.0186 at 10 eV to 0.0016 at 100 eV. Also, the slopes of fitted data decrease with increasing incident energy.

The corresponding DCSs, denoted as $\frac{d\sigma}{d\Omega}$, were obtained from

$$f(K, E) = \frac{\omega}{2}\frac{k_i}{k_f}K^2\left(\frac{d\sigma}{d\Omega}\right) \tag{1}$$

where $f(K, E)$ is GOS, ω is excitation energy, k_i and k_f are the electron momenta before and after the collision and K is given as

$$K^2 = 2E\left[2 - \frac{\omega}{E} - 2\sqrt{1 - \frac{\omega}{E}}\cos\theta\right] \tag{2}$$

where E is the impact energy. DCSs determined from GOSs in this way are inserted in figure 5. In the same figure absolute DCSs at higher scattering angles are shown. As one can see, for 10 eV impact energy the DCS curve has a minimum at 90°. At 20 eV two minima show up, one at 90° and another at 140°. As the energy increases these minima become more pronounced. The first one becomes deeper moving towards smaller scattering angles, from 90° at 20 eV to 70° at 60 eV. At 60 eV the DCS is strongly forward peaked and the intensity of the curve changes six orders of magnitude in the full range of scattering angles.

There are two sources that contribute to the total error for absolute DCS values: the uncertainties in experimental values and uncertainties in normalization procedure. The contribution to the first source arises from statistical errors, uncertainty of angular scale, uncertainty of energy scale and uncertainty of applied effective path-length correction. Averaged statistical error is estimated to be 9%. The angular uncertainty is less than 0.3° and its contribution to the DCS error is slightly larger at small scattering angles. Uncertainty of the energy scale is determined to be 100 meV and the corresponding contribution is larger

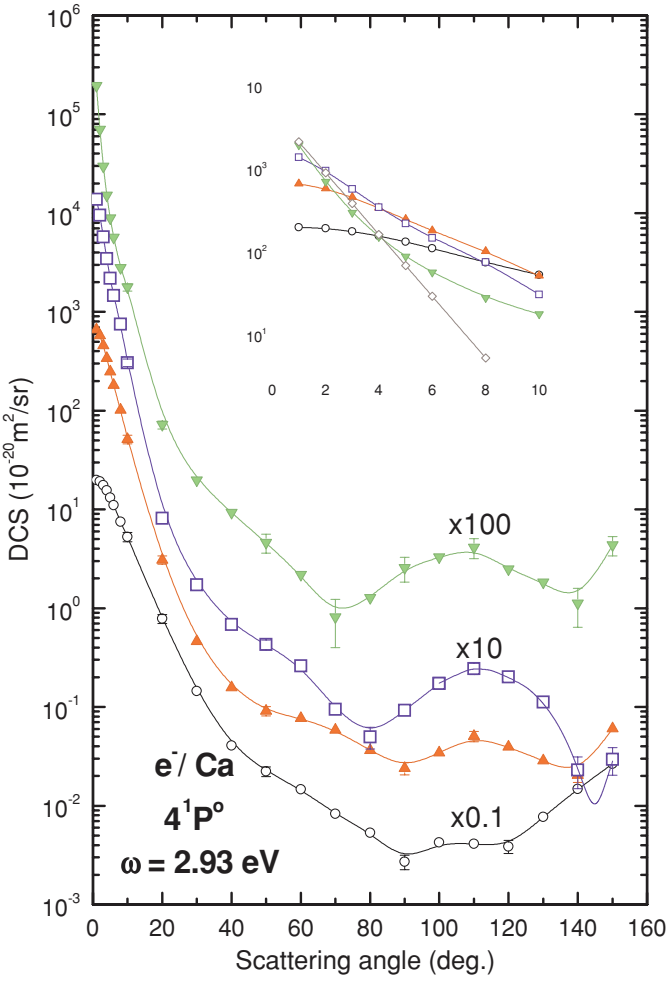

Figure 5. Differential cross sections for excitation of the 4 ^{1}P^o state of Ca: ○, 10 eV; ▲, 20 eV; □, 40 eV; ▼, 60 eV; ◇, 100 eV electron-impact energy. The curves are multiplied by the indicated factors.

M A supplementary data table is available online at stacks.iop.org/JPhysB/37/3571

at smallest impact energy (1% at 10 eV). The error due to the applied geometrical effective path-length correction factor is 5%. Uncertainty in the normalization arises from uncertainty of the OOS value which was determined with 1.7% accuracy and the fitting procedure (leads to an uncertainty between 9% and 15%). The total error for the absolute DCS was determined as the square root of the sum of the particular squared errors.

There are no experimental data to compare with the obtained DCSs. The only comparisons possible are with theoretical data by Srivastava *et al* [29]. Their calculation for DCSs has been carried out in the relativistic distorted-wave approximation for the excitation of calcium from the ground state to the 4 ^{1}P^o for 30, 40 and 60 eV incident electron energies. Our results at 40 eV and 60 eV are compared with these calculated data and presented in figure 6. At 60 eV DCS falls within six orders of magnitude in the angular interval from 1° to 70°. The shape of the angular distribution and the absolute values are in good agreement with the theory in the region from 50° to 150°, but the behaviour of the theoretical and experimental

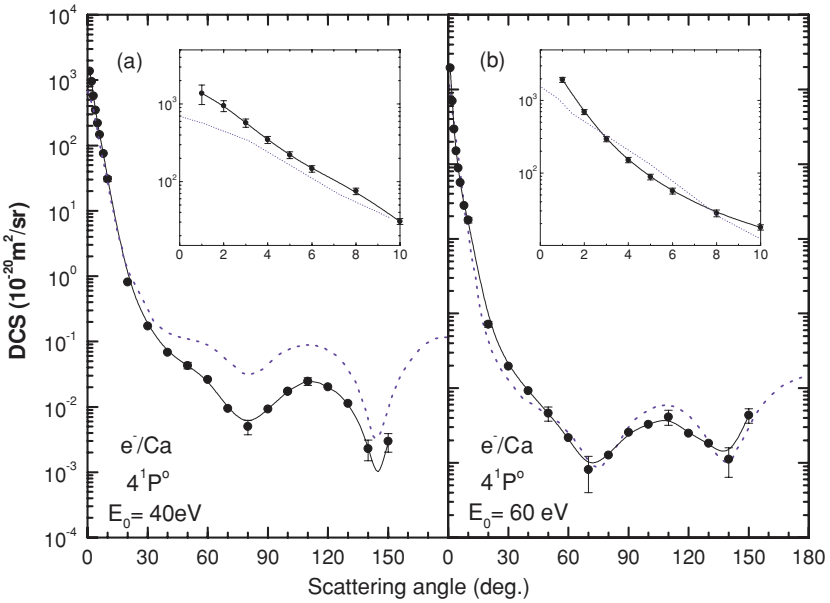

Figure 6. Differential cross sections for excitation of the 4 ^{1}P^o state of Ca at (a) 40 eV and (b) 60 eV electron-impact energy: ●, present results; · · · · · ·, theoretical (RDW) data by Srivastava *et al* [29].

DCSs at smaller scattering angles is slightly different. In a detailed look at the shape one can see disagreement in slope in the angular interval from 0° to 10° (see the inset in figure 6(b)). At 40 eV the agreement is not so good. Theoretical calculation gives generally larger cross sections at scattering angles larger than 20°. At higher angles ($\theta > 40°$) calculated values are higher than experimental ones by a factor of approximately 5. But both the theory and the experiment have the inflection point at 50°, the first local minimum at 80°, the local maximum at 110° and the second minimum between 140° and 150°. If we normalize the maximum at 110° to that calculated at the same angle, then we will reach agreement in shape and the DCS minimum at 80° will coincide. The theory predicts the existence of a second DCS minimum at 145° where an experimental data point was not obtained. The present fitting curve for DCS at this scattering angle was obtained by normalization to the available calculations [29].

The differential cross sections were extrapolated to 0° and 180° in order to determine integrated cross sections: integral (Q_I), momentum transfer (Q_M) and viscosity (Q_V), defined as

$$Q_I = 2\pi \int_0^\pi \sigma(\theta) \sin\theta \, \mathrm{d}\theta \tag{3}$$

$$Q_M = 2\pi \int_0^\pi \sigma(\theta) \left[1 - \left(1 - \frac{\omega}{E_0}\right)^{1/2} \cos\theta\right] \sin\theta \, \mathrm{d}\theta \tag{4}$$

$$Q_V = 2\pi \int_0^\pi \sigma(\theta) \left[1 - \left(1 - \frac{\omega}{E_0}\right) \cos^2\theta\right] \sin\theta \, \mathrm{d}\theta. \tag{5}$$

For 40 eV and 60 eV electron-impact energies, extrapolation in the range $150° < \theta \leqslant 180°$ was based upon calculation by Srivastava *et al* [29]. At 10 eV and 20 eV this procedure was

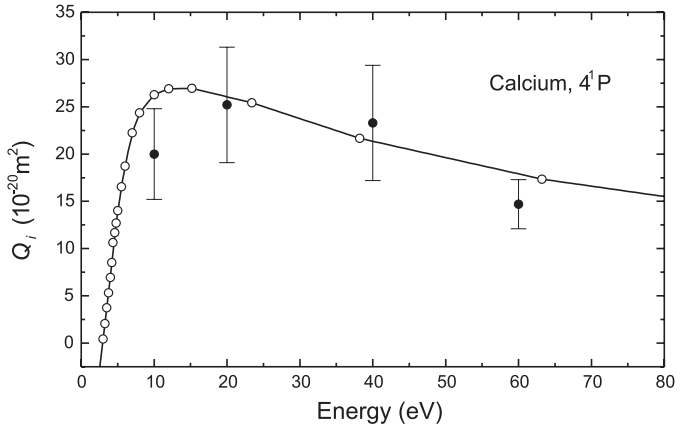

Figure 7. Integral cross sections for the 4 ^{1}P^o state of the calcium atom: ●, present results; ○, results by Ehlers and Gallagher [14].

done by fitting the measured values using polynomial functions. Extrapolation to 0° was made by using the corresponding fitting curves for the GOSs. Calculated 4 ^{1}P integral cross sections are shown in figure 7, where they are compared with integral cross sections determined by Ehlers and Gallagher [14]. The shapes of Q_I of both experimental studies are very similar except we did not perform measurements at energies between 10 and 20 eV where Ehlers and Gallagher [14] obtained a maximum (at 15.19 eV). Their results generally agree with ours but they are still above our quoted error bars at 60 eV and 10 eV where they overestimated our Q_I by about 30%. A possible reason for this disagreement could be the fact that Ehlers and Gallagher [14] measured total cross sections for excitation to the 4 ^{1}P level including contribution from excitation to higher levels which cascade through the 4 ^{1}P. They estimated that cascade processes contributed 15–30% to their results at low energies.

4. Conclusions

Our aim was to investigate electron excitation of the 4 ^{1}P^o resonant state of calcium atom. We have obtained differential cross sections as well as integral, momentum transfer and viscosity cross sections. The results were obtained for 10, 20, 40 and 60 eV in the angular range from 1° to 150° and for 100 eV at small scattering angles. To the best of our knowledge, the results reported in this paper are the first experimental DCSs for calcium at impact energies from 10 to 100 eV. The absolute DCS scale was obtained by normalization of generalized oscillator strengths at small scattering angles up to 10° to the optical oscillator strength. Comparison with theoretical results shows that generally good agreement exists between experiment and available calculations at higher energy and larger scattering angles. At lower electron impact energies there are no data to compare with. There is a need for more theoretical and experimental work on excitation processes for the resonant and higher excited states in the energy range considered in this paper. We hope that our results will stimulate further scattering studies of the calcium atom.

Acknowledgment

This work has been carried out within project OI 1424 financed by MNZŽS of Republic Serbia.

References

[1] Smith G 1988 *J. Phys. B: At. Mol. Opt. Phys.* **21** 2827
[2] Dimitrijević M S and Sahal-Brechot S 1999 *Astron. Astrophys. Suppl.* **140** 191
[3] Liang Gui-Yun, Bian Xia and Zhao Gang 2004 *Chin. Phys.* **13** 0891
[4] Holweger H 1972 *Solar. Phys.* **25** 14
[5] Thoren P 2000 *Astron. Astrophys.* **358** L21
[6] Chmielewski Y 2000 *Astron. Astrophys.* **353** 666
[7] Udem Th, Diddams S A, Vogel K R, Oates C W, Curtis E A, Lee W D, Itano W M, Drullinger R E, Bergquist J C and Hollberg L 2001 *Phys. Rev. Lett.* **86** 4996
[8] Oates C W, Bondu F, Fox R W and Hollberg L 1999 *Eur. Phys. J.* D **7** 449
[9] Oates C W, Curtis E A and Hollberg L 2000 *Opt. Lett.* **25** 1603
[10] Kisters Th, Zeiske K, Reihle F and Helmcke J 1994 *Appl. Phys.* B **59** 89
[11] Kurosu T, Zinner G, Trebst T and Reihle F 1998 *Phys. Rev.* A **58** R4275
[12] Binnewies T, Wilpers G, Sterr U, Riehle F, Helmcke J, Mehlstaubler T E, Rasel E M and Ertmer W 2001 *Phys. Rev. Lett.* **87** 3002
[13] Bauch A and Telle H R 2002 *Rep. Prog. Phys.* **65** 789
[14] Ehlers V J and Gallagher A 1973 *Phys. Rev.* A **7** 1573
[15] Zohny E I M, El Fayoumi M A K, Hamdy H, Beyer H-J, Eid Y A, Shahin F and Kleinpoppen H 1989 *16th Int. Conf. on the Physics of Electronic and Atomic Collisions (New York, 1989), Abstracts of Contributed Papers* ed A Dalgarno, R S Freud, M S Lubell and T B Lucatorto p 173
[16] Chwirot S, Srivastava R, Dyl D and Dygdala R S 1996 *J. Phys. B: At. Mol. Opt. Phys.* **29** 5919
[17] Dyl D, Dziczek D, Piwinski M, Gradziel M, Srivastava R, Dygdala R S and Chwirot S 1999 *J. Phys. B: At. Mol. Opt. Phys.* **32** 837
[18] Law M R and Teubner P J O 1995 *J. Phys. B: At. Mol. Opt. Phys.* **28** 2257
[19] Murray A J and Cvejanović D 2003 *J. Phys. B: At. Mol. Opt. Phys.* **36** 4889
[20] Cvejanović D and Murray A J 2003 *J. Phys. B: At. Mol. Opt. Phys.* **36** 3591
[21] Murray A J and Cvejanović D 2003 *J. Phys. B: At. Mol. Opt. Phys.* **36** 4875
[22] Pejčev V, Ottley T W, Rassi D and Ross K J 1978 *J. Phys. B: At. Mol. Opt. Phys.* **11** 531
[23] Feuerstein B, Zatsarinny O I and Mehlhorn W 2000 *J. Phys. B: At. Mol. Opt. Phys.* **33** 1237
[24] Bizau J M, Gerard P, Wuilleumier F J and Wendin G 1987 *Phys. Rev.* A **36** 1220
[25] Ueda K, Kabachnik N M, West J B, Ross K J, Beyer H J, Hamdy H and Kleinpoppen H 1998 *J. Phys. B: At. Mol. Opt. Phys.* **31** 4331
[26] Beyer H J, West J B, Ross K J and De Fanis A 2000 *J. Phys. B: At. Mol. Opt. Phys.* **33** L767
[27] Hamdy H, Beyer H J and Kleinpoppen H 1990 *J. Phys. B: At. Mol. Opt. Phys.* **23** 1671
[28] Stevenson M and Crowe A 2004 *J. Phys. B: At. Mol. Opt. Phys.* **37** 2493
[29] Srivastava R, Zuo T, McEachran R P and Stauffer A D 1992 *J. Phys. B: At. Mol. Opt. Phys.* **25** 3709
[30] Zuo T, McEachran R P and Stauffer A D 1991 *J. Phys. B: At. Mol. Opt. Phys.* **24** 2853
[31] Muktavat K, Srivastava R and Stauffer A D 2002 *J. Phys. B: At. Mol. Opt. Phys.* **35** 4797
[32] Predojević B, Šević D, Pejčev V, Marinković B P and Filipović D M 2003 *J. Phys. B: At. Mol. Opt. Phys.* **36** 2371
[33] Brinkman R T and Trajmar S 1981 *J. Phys. E: Sci. Instrum.* **14** 245
[34] Felfli Z and Msezane A Z 1998 *J. Phys. B: At. Mol. Opt. Phys.* **31** L165
[35] Tošić S, Šević D, Pejčev V, Filipović D M and Marinković B P 2003 *23rd Int. Conf. on Photonic Electronic and Atomic Collisions (Stockholm, 2003), Abstracts of Contributed Papers* ed J Anton, H Cederquist, M Larsson, E Lindroth, S Mannervik, H Schmidt and R Schuch Tu050
[36] Avdonina N B, Felfli Z and Msezane A 1997 *J. Phys. B: At. Mol. Opt. Phys.* **30** 2591
[37] Kelly F M and Mathur M S 1980 *Can. J. Phys.* **58** 1416